

## High-Intensity Flash X-Ray Source for HERMES III\*

T.W.L. Sanford, J. A. Halbleib,  
W. H. McAtee, and R. C. Mock

Sandia National Laboratories  
Albuquerque, NM 87185

### Abstract

The design of an intense source of flash x-rays that delivers a measured peak dose and dose rate of 370 krad(Si) and  $3.5 \times 10^{13}$  rad(Si)/s over a useful area of 80 cm<sup>2</sup> without target destruction is described, and measurements are compared with predictions of a numerical model. The quality of the agreement gives credibility to the measurements, validates the main assumptions of the model, and gives insight into the generation and transport of the electron/photon cascade within the source.

### Introduction

HERMES III is a 19-MV, 700-kA, 25-ns pulsed electron accelerator [1] that produces intense bremsstrahlung doses and dose rates over large areas, for the study of nuclear radiation effects induced by  $\gamma$ -rays. The standard EPA (extended planar-anode) diode delivers peak dose and dose rate of 100 krad(Si) and  $5 \times 10^{12}$  rad(Si)/s over a useful area (area where the dose is greater than 50% of the peak dose) of 1000 cm<sup>2</sup> [2]. This diode has been used successfully as the baseline radiation source since the accelerator was commissioned 3 years ago.

In this paper, we describe a method of focusing the radiation in order to obtain much higher doses and dose rates over smaller areas. The concept is illustrated in Figure 1, where a low pressure gas cell (3 torr N<sub>2</sub>) is introduced between the anode window and bremsstrahlung target. In the gas, the high inductive electric fields generated by the beam rapidly charge-neutralize and partially current-neutralize the incident beam, resulting in ballistic propagation. The introduction of the gas cell thus permits the annular beam to impact the target at a small radius, with little dispersion from self-fields. With this design, the radiation dispersion at the focus is minimized and the formation of an anode plasma at the upstream surface of the target due to high energy-deposition from the incident beam is no longer an issue, because the surface is inside the gas cell.

\*This work was supported by the United States Department of Energy under contract DE-AC04-76 DP000789.

In the following, we describe the optimization of this configuration as a function of anode-window material, target composition, gas-cell length, and beam-stabilizing mechanism. The results are compared with a two-dimensional numerical model [3] that uses the MAGIC computer code [4] to calculate the electron flow in the azimuthally symmetric AK gap and the CYLTRAN computer code of the ITS system [5] to calculate the subsequent ballistic transport in the gas cell and the electromagnetic shower in the target and downstream radiation diagnostics.

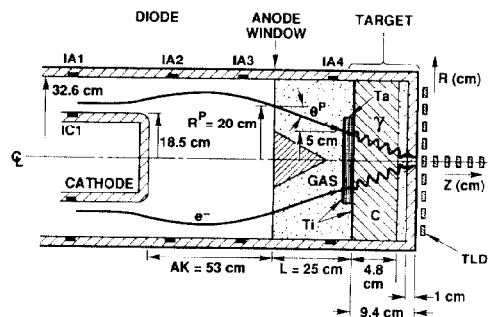
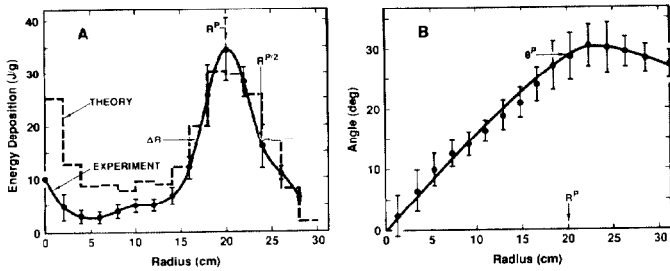


Figure 1. Schematic of high-intensity source

The experimental arrangement utilizes or modifies the existing hardware developed for the EPA diode. The operation of the accelerator and modeling are similar to that described in References 2 and 3. Briefly, sets of current shunts (IC1, IA1, . . . IA4) are used to measure current flow in the diode and gas cell, TLDs (thermoluminescent dosimeters) along the Z-axis measure the axial position of the radiation focus, and a 100-element graphite calorimeter (which replaces the target) in combination with a 48-Element TLD array at Z=0 cm are used to measure the radial energy-deposition profile and mean angle of incidence ( $\theta^P$ ) at the anode window and target, respectively. The model uses the time-integrated coupled radial and angular distribution at the anode window from the steady-state MAGIC simulation of electron flow at 20 MV (Figure 2), together with the measured time-integrated kinetic-energy distribution of the electrons, as input to CYLTRAN. The model calculations of dose downstream of the target are all normalized to the dose-area product measured in the TLD array at Z=0 cm.



**Figure 2.** (A) Comparison of measured (for a 53-cm AK gap and solid cathode tip) and calculated (for a 60-cm AK gap and annular cathode tip) radial electron energy deposition at anode window. Errors correspond to RMS variation measured along  $\pm X$  and  $\pm Y$  axes at the same  $R$ . (B) Corresponding calculated angular distribution. Errors correspond to RMS variation in the associated 2-cm radial bin.

### Anode window and target

For the high-intensity source, we use the EPA diode with a 53-cm AK gap and solid cathode tip. The gap allows the beam to enter the gas cell with a measured radius and convergence angle of  $20 \pm 0.5$  cm and  $30 \pm 3^\circ$ , respectively. Under these conditions, the incident beam imparts an energy deposition of only 30 J/g(C) at the anode window (Figure 2), which is an order of magnitude below that necessary to produce an anode plasma [6]. The solid tip minimizes the on-axis current density and concentrates the bulk of the current density at large radius [3].

At the input and exit of the gas cell, a 0.2-mm-thick aluminum anode window and a 1.5-mm-thick tantalum converter are used, respectively, to maximize the radiation dose on axis. By using the thinner window of lower  $Z$  relative to the 0.3-mm-thick titanium window of Reference 2, the multiple-Coulomb-scattering of the incident beam is kept below the intrinsic  $\pm 4^\circ$  beam dispersion. Thus, scattering of the beam in the window does not contribute significantly to the dispersion of the annular beam at the target. Secondly, CYLTRAN calculations show that  $\sim 1.5$  mm, instead of the 3 mm of tantalum in the Ti/Ta/C target designed for bremsstrahlung production with the EPA diode, maximizes the radiation at the focus, while still preventing primary electrons from traversing the graphite absorber. Accordingly, the tantalum thickness of the EPA target is reduced to 1.5 mm for this application.

### Gas-Cell Length

The radius ( $R^P$ ) of the beam measured at the target for a gas cell length of 25 cm and 30 cm coincides with that projected from the measured angle ( $\theta^P$ ) at the anode window (Figure 3). Accordingly, in the model, the self-fields of the beam in the gas are ignored, and the propagation of the beam in the gas and subsequent electromagnetic shower in the target and downstream

TLDs are modeled using CYLTRAN. This model shows that a gas-cell length ( $L$ ) of  $\sim 25$  to 30 cm maximizes the dose at the radiation focus, in agreement with that expected geometrically (Figure 3) and that measured (Figure 4). Additionally, the measured HWHM of the axial and radial radiation profiles (Figure 5A) are in agreement with those calculated, showing that there are no new effects contributing significantly to the dispersion of the radiation focus. The difference between measured and calculated peak doses (Figure 4) is likely due to the three-dimensional and time-dependent effects not included in the model.

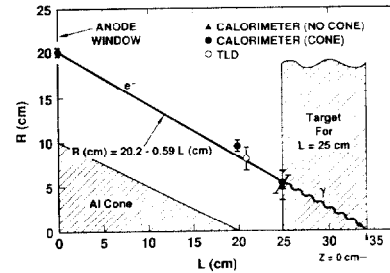


**Figure 3.** ( $\bullet$ ,  $\blacktriangle$ ) Radius of annular electron beam ( $R^P$ ) measured in calorimeter as a function of gas-cell length ( $L$ ). (o) Radius of annular radiation beam generated at anode window for  $L=0$  cm and measured in TLD array 21-cm downstream of anode window.

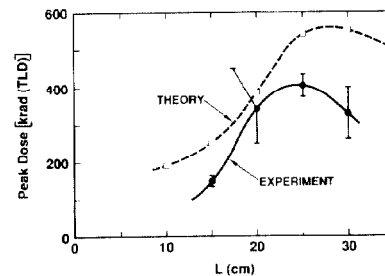


**Figure 4.** Comparison of measured and calculated peak dose at radiation focus as a function of gas-cell length ( $L$ ).

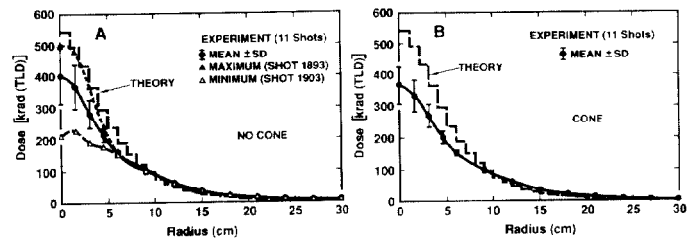


**Figure 5.** A comparison of measured and calculated radiation dose profile at radiation focus ( $Z=0$ ) for  $L=25$  cm. ( $\bullet$ ) mean and RMS variation about mean,  $\blacktriangle$  maximum dose profile and  $\triangle$  minimum dose profile measured in radial TLD array at  $Z=0$  for 11 shots. (A) Conical structure is not present. (B) Conical structure is present.

Such variations are observed when the calculated radial electron energy deposition is compared with that measured at the target (Figure 6). The variation measured with azimuth or between shots is more than a

factor of two times the mean at a given radius. Accordingly, the target, in order to survive, is designed to handle depositions over wide excursions. For our high-intensity source, the thickness of the tantalum laminations is reduced from the 0.051 mm thickness used in the EPA target to 0.013 mm in order to increase the threshold for spalling the tantalum from 85 J/g to 340 J/g. Under these conditions, the target has survived over 50 shots without destruction.

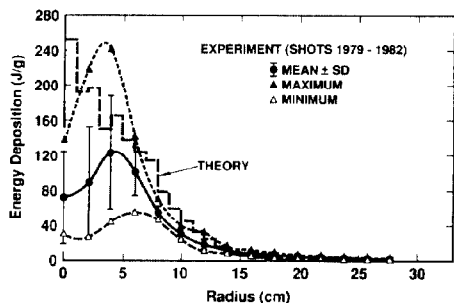


**Figure 6.** Comparison of measured and calculated surface energy deposition at the target as a function of radius for  $L=25$  cm. Conical structure is in place for the measurements. (•) mean and RMS variation about mean, ▲ maximum, and △ minimum deposition for measurements made along  $\pm X$  and  $\pm Y$  axes at same radius for sequential shots.

### Stability

At the  $L=25$  cm optimum, a peak dose of  $402 \pm 88$  krad(TLD) is measured (Figure 5A). It occurs at the downstream face of the vacuum chamber as expected. The RMS variation in the peak dose is  $\pm 22\%$ . It varies by a factor of 2.4 between extremes when measured over 11 shots. The variation in peak-dose is strongly correlated with the  $\pm 1.5$  cm shot-to-shot variation in the axial position of the focus, and the magnitude of the variation in peak-dose is in rough agreement with the decrease expected when the focus occurs farther downstream. About half of the variation in the position of the axial focus is directly attributed to the variation in the mean  $R^P$  and  $\theta^P$  at the input to the gas cell due to the measured  $\pm 0.3$ -MeV shot-to-shot variation in peak voltage. The remainder may be due to 3-D effects.

By introducing the coaxial conical structure shown in Figures 1 and 3, a weak magnetic restoring force is applied to the beam due to the induced net currents flowing on the cone. Experimentally, the application of the cone does not alter the mean position of the beam at the target (Figure 3). It does, however, reduce the RMS variation in the peak dose from  $22 \pm 3.5\%$  to  $16 \pm 2.5\%$  (Figure 5B).

Examination of Figure 4 shows that additional stability in peak-dose due to variation in focal position might be gained by adjusting the focus such that it falls a few centimeters inside the downstream face of the vacuum chamber. Because of the higher energy density at the upstream face of the target, however, the

spallation threshold of the tantalum is exceeded. At present, this additional stabilizing potential is only applied minimally (Figure 3).

### Conclusion

Introducing a low-pressure gas cell with a coaxial cone between the anode window and target of the EPA diode permits a peak-dose of 370 krad(Si) and corresponding peak dose-rate [7] of  $\sim 3.5 \times 10^{13}$  rad(Si)/s (with  $\pm 16\%$  shot-to-shot variation) to be achieved over a useful area of  $\sim 80$  cm<sup>2</sup> without destruction of the radiation source (Figure 5B). The agreement between the radiation profiles measured and calculated gives credibility to both, as well as to the approximations made in the model.

### Acknowledgments

We thank J. W. Poukey for calculating the MAGIC distribution used in the model; R. L. Westfall and the HERMES III crew for technical support; J. J. Ramirez, J. E. Maenchen, J. E. Powell, W. Beezhold, and J. R. Lee for vigorous support of this research; and D. E. Beutler for reviewing this paper.

### References

- [1] J. J. Ramirez, K. R. Prestwich, D. L. Johnson, J. P. Corley, G. J. Denison, J. A. Alexander, T. L. Franklin, P. J. Pankuch, T. W. L. Sanford, T. J. Sheridan, L. L. Torrison, and G. A. Zawadzka, *Digest of Technical Papers of the 7th IEEE Pulse Power Conference*, edited by R. White and B. H. Bernstein (IEEE, New York, 1989), pp. 26-31.
- [2] T. W. L. Sanford, J. A. Halbleib, and R. C. Mock, *IEEE Trans Nucl Sci*, vol. NS-37, No. 6, P. 1762, 1990.
- [3] T. W. L. Sanford, J. A. Halbleib, J. W. Poukey, G. T. Baldwin, G. A. Carlson, W. A. Stygar, G. A. Mastin, T. Sheridan, R. Mock, J. A. Alexander, E. R. Brock, and C. O. Landron, *J Appl Phys*, vol. 67, p. 1700, 1990.
- [4] B. Goplen, R. E. Clark, J. McDonald, W. M. Bollen, "Users Manual for MAGIC," Mission Research Corporation Report No. MRC/WDC-R-068, Alexandria, VA (September 1983).
- [5] J. A. Halbleib, in *Monte Carlo Transport of Electrons and Photons*, edited by T. M. Jenkins, W. R. Nelson, and A. Rindi (Plenum Publishing Corporation, New York, 1988), pp. 249-284.
- [6] T. W. L. Sanford, J. A. Halbleib, J. W. Poukey, A. L. Pregoner, R. C. Pate, C. E. Heath, R. Mock, G. A. Mastin, D. C. Ghiglia, T. J. Roemer, P. W. Spence, and G. A. Proulx, *J Appl Phys*, vol. 66, p. 10, 1989.
- [7] T. W. L. Sanford, J. A. Halbleib, D. E. Beutler, W. H. McAtee, R. C. Mock, and D. P. Knott, to be presented at 28th International Nuclear and Space Radiation Effects Conference (San Diego, CA, July 15-19, 1991).